

Comparison of Reconstruction Algorithms for Images from Sparse-Aperture Systems

J.R. Fienup,^a □ D. Griffith,^b L. Harrington,^b A.M. Kowalczyk,^b J.J. Miller,^b and J.A. Mooney^c

^aInstitute of Optics, Wilmot 410, University of Rochester, Rochester, NY 14627

^bVeridian Systems, P.O. Box 134008, Ann Arbor, MI 48113-4008

^cEastman Kodak Company, 1447 St. Paul St., Rochester, NY 14650

ABSTRACT

Telescopes and imaging interferometers with sparsely filled apertures can be lighter weight and less expensive than conventional filled-aperture telescopes. However, their greatly reduced MTF's cause significant blurring and loss of contrast in the collected imagery. Image reconstruction algorithms can correct the blurring completely when the signal-to-noise ratio (SNR) is high, but only partially when the SNR is low. This paper compares both linear (Wiener) and nonlinear (iterative maximum likelihood) algorithms for image reconstruction under a variety of circumstances. These include high and low SNR, Gaussian noise and Poisson-noise dominated, and a variety of aperture configurations and degrees of sparsity. The quality metric employed to compare algorithms is image utility as quantified by the National Imagery Interpretability Rating Scale (NIIRS). On balance, a linear reconstruction algorithm with a power-law power-spectrum estimate performed best.

Keywords: Image reconstruction, sparse apertures, deconvolution, image restoration, MTF, image quality, Wiener filter, power spectrum estimation, maximum likelihood

1. INTRODUCTION

Applications such as NASA's terrestrial planet finder¹ have a need for imaging with ultra-fine angular resolution, which requires telescopes or imaging interferometers having large diameters. In such cases, scaling up the size of a conventional telescope, such as the Hubble Space Telescope, is impractical because it is too heavy and expensive. An alternative is to use a sparse-aperture telescope -- one with most of the aperture missing -- or to use an interferometer. As long as the optical transfer function (OTF, which is the autocorrelation of the aperture function) is filled, one can achieve a resolution as good as that from a filled-aperture telescope. The price one pays, however, is that the modulation transfer function (MTF, the magnitude of the OTF) is greatly suppressed for sparse apertures. Boosting of the MTF, to restore the proper relationships of the spatial frequencies, increases the noise; hence, the presence of noise degrades the imagery of sparse-aperture telescopes many times more than it degrades imagery from conventional telescopes. This can be overcome by increasing the signal-to-noise ratio (SNR) by using longer integration (exposure) times.^{2,3} Practical limitations on the exposure times often prevent the sufficiently high SNR necessary to obtain full recovery at the diffraction-limited resolution.

As illustrated in Figure 1, initially the imagery from sparse-aperture telescopes is of low contrast and blurred out. With high SNR, an image indistinguishable from the original diffraction-limited image can be reconstructed, but when even a modest amount of noise is present, the reconstructed image suffers. The degree of sensitivity to the noise increases as the fill factor of the telescope decreases. The fill factor is defined as the area of the clear aperture divided by the area of a circular aperture giving the same resolution.

□ fienup@optics.rochester.edu

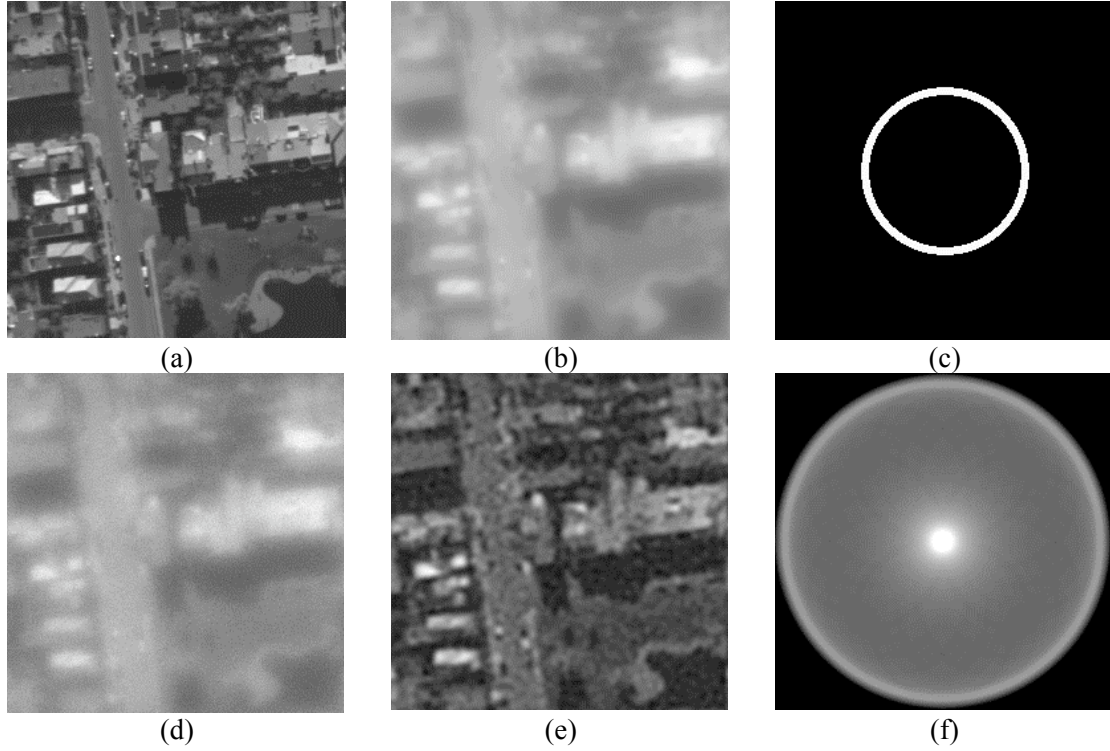


Figure 1. Example of imaging through a sparse aperture.² (a) Original aerial photograph, (b) diffraction-limited image through annular aperture, (c) annular aperture, with 24% fill factor, (d) raw image [photon noise applied to (b)] with SNR = 32, (e) Wiener-Helstrom-filtered version of (d), (f) MTF of annular aperture (square root taken to compress large dynamic range).

This paper explores the question: what kind of reconstruction algorithm is best to use for images from sparse apertures? In Section 2 we review two classes of algorithms: linear (Wiener filters) and nonlinear (maximum-likelihood). In Section 3 we show experimental results. In Section 4 we analyze the noise to understand the experimental results. In Section 5 we present our conclusions.

2. RECONSTRUCTION ALGORITHMS

Linear reconstruction algorithms attempt to deconvolve the effect of the sparse aperture by differential boosting of spatial frequencies in the Fourier transform plane. Nonlinear algorithms attempt to maximize a log-likelihood ratio using an iterative or recursive nonlinear optimization algorithm.

2.1 Wiener filter

If we model the raw images as

$$g(x,y) = f(x,y) \ast s(x,y) + n(x,y), \quad (1)$$

where $f(x,y)$ is the diffraction-limited image (or the object or the scene), $s(x,y)$ is the point-spread function (PSF), \ast denotes convolution, and $n(x,y)$ is the noise, then in the Fourier domain we have

$$G(u,v) = F(u,v)S(u,v) + N(u,v), \quad (2)$$

where the functions represented by capital letters are the Fourier transforms of the functions represented by the corresponding lower-case letters. $S(u,v)$ is the optical transfer function (OTF). The suppression of the Fourier data by the OTF (same as the MTF when there are no aberrations) of a sparse aperture is seen by the low values of the MTF in the example of Figure 2.

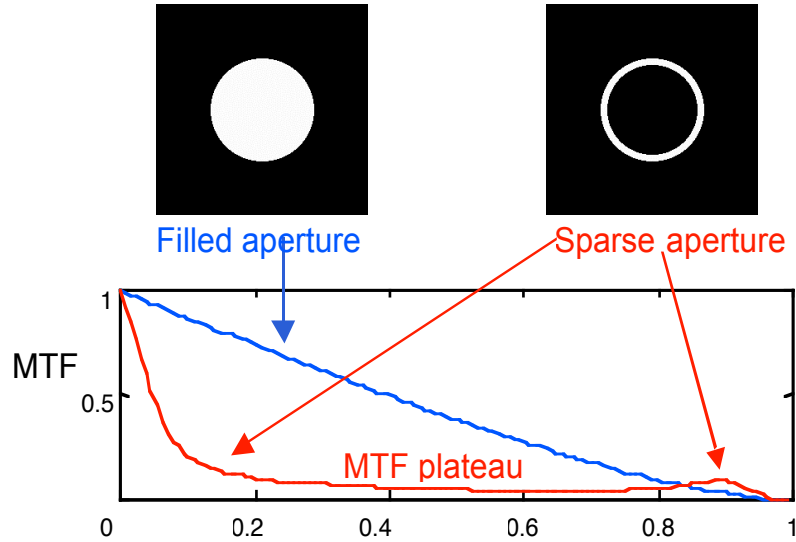


Figure 2. A filled circular aperture, a sparse annular aperture, and their MTFs.²

Wiener-Helstrom filtering⁴ (or “Wiener filtering” for brevity) multiplies this Fourier data by the filter function

$$W(u,v) = \frac{S^*(u,v)}{|S(u,v)|^2 + c \frac{\sigma_N}{\sigma_o}(u,v)} \quad (3)$$

and inverse transforms to arrive at the reconstructed image. Here c is a positive constant, and $\frac{\sigma_N}{\sigma_o}(u,v)$ is the ratio of the power spectrum of the noise (which can be well approximated as a constant) to the power spectrum of the object. Using $c = 1.0$ gives the minimum mean-squared error reconstruction, but smaller values of c are usually preferred, to give increased edge sharpness at the expense of increased noise. Since the power spectrum of the object is unknown, it must be estimated. Often researchers use an estimate that is a constant, even though the power spectrum typically varies from low to high spatial frequencies by orders of magnitude. We have found⁵ that typically the object’s mean Fourier magnitude (the square of which is the power spectrum) can be approximated by a power law of the form $A r^{\alpha}$, where A and α are constants and $r = \sqrt{u^2 + v^2}$ is the radial component of spatial frequency. The parameter α is sometimes referred to as the fractal dimension of the object. A , α , and the noise level can be estimated by curve-fitting the model to the given Fourier data.⁵ Another possibility is to estimate the power spectrum by curve-fitting, perform the Wiener filter, and use the resultant Fourier data as a new estimate for the power spectrum of the object. This process can be repeated in a second (or more) recursion. We refer to this as the recursive Wiener filter.

2.2 Nonlinear Maximum-Likelihood Reconstruction

A second approach to image reconstruction is to maximize the log-likelihood function to determine the object that, when convolved with the PSF, gives the best agreement with the measured image, given the statistics of the noise. For additive Gaussian noise, as would come from read noise, this reduces to the Wiener filter. For Poisson noise (shot noise), as one would have when photon noise dominates, there is no closed-form solution for the estimate, and it is typically found via iterative numerical algorithms.^{6,7}

3. EXPERIMENTAL RESULTS

In one set of experiments we started with an aerial photograph of a city area (the Presidio in San Francisco, courtesy of Jet Propulsion Laboratory), convolved it with the point spread function due to an annular aperture with a fill factor of 24%, normalized the mean value to 1,000, and simulated photon noise. Hence the average SNR across the image was the square root of 1,000, or about 32. The pristine image and the simulated noisy image through the sparse aperture are shown in Figure 3(a) and (b). Images reconstructed from Veridian System's version of a maximum likelihood (ML) algorithm and Wiener filter are also shown in Figure 3. For the ML algorithm, increasing the number of iterations increases the edge sharpness but also increases the noise. (A graying of the edges of the reconstructed images is a result of a guard-band to avoid edge artifacts.) Similarly, for the Wiener filter, decreasing the Wiener constant, c , increases the edge sharpness as well as the noise. The value of $c = 1.0$, shown in Figure 3(f), gives the image having the smallest squared error; however, most people prefer the images having smaller values of c , preferring the sharper edges despite the increased noise. The visually best image reconstructed from the ML algorithm appears to be sharper with less noise amplification than the best image reconstructed from the Wiener filter. From the point of view of image quality, the ML algorithm is clearly superior in this circumstance (high contrast image with only photon noise of moderate SNR). This should not be surprising because the ML algorithm explicitly takes into consideration the Poisson statistics of the noise, whereas the Wiener filter assumes Gaussian noise, which is not the case here. On the other hand, the Wiener filter is many times faster than the ML algorithm, requiring only two fast Fourier transforms (FFTs), whereas the ML algorithm requires dozens or hundreds of FFTs. When the number of photons per pixel was increased to 10,000, giving an SNR of 100, the images shown in Figure 4 resulted. In this case, the image from the ML algorithm and the Wiener filter were comparable. For higher SNRs, we found that the ML algorithm has no advantage over a Wiener filter.

In a second set of experiments, we simulated numerous cases for a variety of scenarios. Aperture types included annular, Golay-6, and tri-arm (Y-shaped). SNRs included values of 6, 24, and 75. Fill factors were 10% and 30%. Scenes included images of an airport, a ship at dock, and an industrial area. 216 images were simulated with various combinations of parameters. The effect of atmospheric haze was added, assuming a 19-km atmosphere, computed using Modtran 4.0. The number of haze photons was comparable to the number of signal photons. Photon noise was simulated as well as 50 photoelectrons rms of detector noise. On these images, different combinations of algorithms were run, including Veridian Systems' (VS) version of the ML algorithm, Edward Meinel's version of the ML algorithm, VS's Wiener filter (with power-law power spectrum estimation), and Eastman Kodak's Wiener filter (using a constant power spectrum). For the VS ML algorithm, images were compared after several different numbers of iterations, and the one that appeared best was saved and referred to as the baseline ML image. Also saved was one with significantly fewer iterations, giving a less aggressively sharpened image (referred to as the weaker version), and a third with significantly greater iterations, giving a more aggressively reconstructed image (referred to as the stronger version). For the VS Wiener filter, we chose Wiener constants, $c = 0.2$ for the baseline image, 0.6 for the weaker version, and 0.05 for the stronger version. The value of Eastman Kodak's constant power spectrum was chosen by reconstructing with several values and choosing the one that was visually best. The quality of the imagery

was judged according to the NIIRS scale.⁸ Each unit on the NIIRS scale is worth an additional factor of two in resolution.

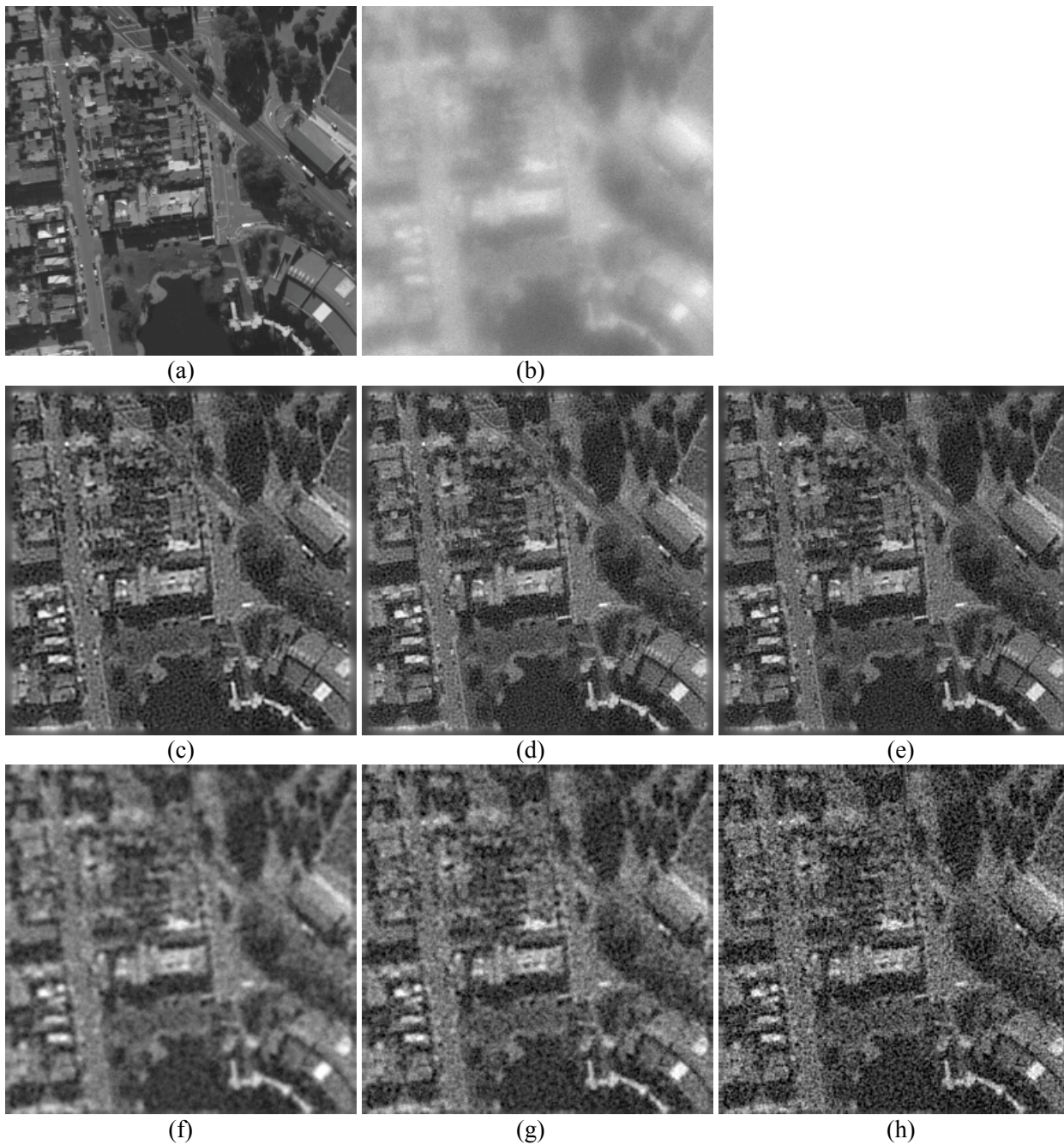


Figure 3. Simulated and reconstructed images. (a) Pristine image, (b) noisy image through sparse aperture, with 1,000 photons per pixel (c) ML 100 iterations, (d) ML 200 iterations, (e) ML 500 iterations, (f) Wiener $c = 1.0$, (g) Wiener $c = 0.3$, (h) Wiener $c = 0.1$.

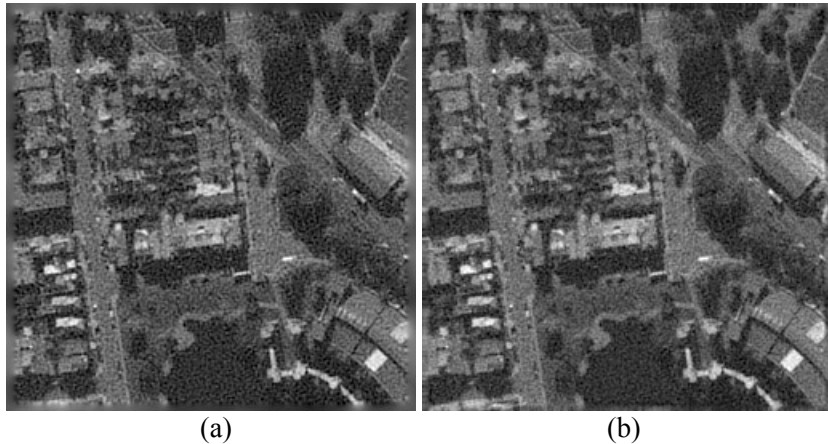


Figure 4. Reconstructed images for 10,000 photons per pixel. (a) ML 500 iterations, (b) Wiener $c = 0.3$.

For the second set of experiments, the results were very different than for the first set of experiments. In the second, more realistically simulated set, the Wiener filter resulted in image quality slightly better than the ML algorithm over-all, by 0.13 NIIRS, according to an analysis of variance (ANOVA). Of course, the Wiener filter was much faster as well. The Wiener filter produced as good or better imagery than the ML algorithm for high SNR as well as for low SNR, for high (30%) fill factor as well as for low (10%) fill factor, for all three aperture types, and for all three scene types.

We also found that on average the Wiener filter using the power-law power-spectrum estimate, with $c = 0.2$, produced images of slightly better quality (by 0.08 NIIRS levels) than using a handpicked constant power spectrum or using the recursive Wiener filter. The power-law Wiener filter has the additional advantage of being completely automated, with no human intervention.

4. ANALYSIS

In this section, we provide a noise analysis, which we believe helps to explain why the Wiener filter could provide image quality comparable to that of the ML algorithm. The variance of the noise per pixel is given by

$$\sigma_N^2 = n_s + n_b + \sigma_r^2, \quad (4)$$

where n_s is the mean number of photons per pixel from the desired signal (the ground), n_b is the number of photons from the haze bias, and σ_r^2 is the variance of the read noise, which was $2,500 = 50^2$ for our simulations. An important issue is that Poisson noise and Gaussian noise have similar probability distributions only if the standard deviation of the image with respect to its mean is substantial. Although the haze noise is Poisson, since the haze level is a constant, it has practically the same statistics as Gaussian noise whenever the number of haze photons is above 16 or so. Hence, the haze noise is indistinguishable from Gaussian noise. Suppose that the mean number of photons from the desired signal is equal to the number of photons from the haze. For this case, the middle curve in Figure 5(a) shows the ratio of the amount of photon noise (from the desired signal) relative to the total noise, and the middle curve in Figure 5(b) shows the SNR for all noise sources. From this we see that when there are enough photons so that the photon noise from the object becomes a large fraction of the total noise, then the SNR is also high. As shown earlier, when the SNR is high enough, then the ML algorithm and the Wiener filter produce similar reconstructions. The upper and

lower curves in Figure 5(a) and (b) are for haze levels that are 1/3 of and 3 times the signal level, respectively.

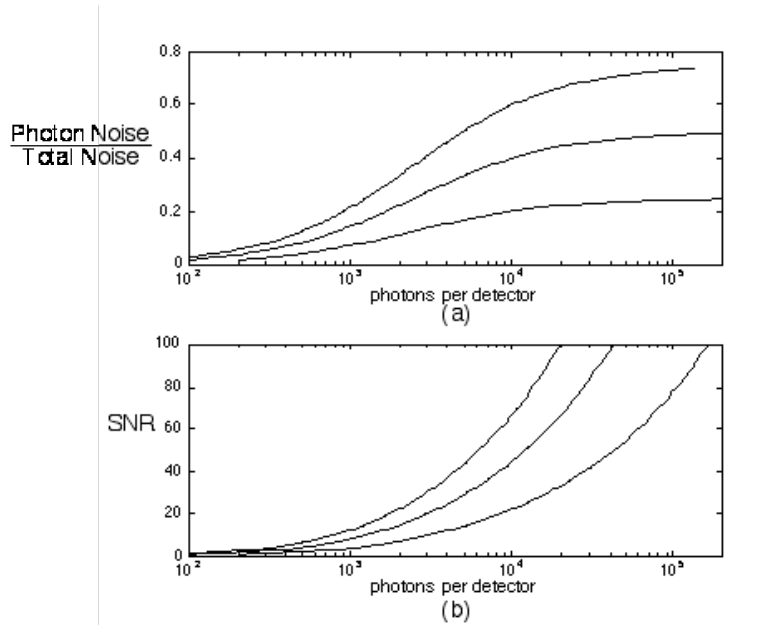


Figure 5. (a) Ratio of photon noise to total noise versus number of photons per pixel. (b) SNR versus number of photons per pixel. Upper curves: signal/haze = 3, middle curves: signal/haze = 1, lower curves: signal/haze = 1/3.

5. CONCLUSIONS

We compared two classes of algorithms, nonlinear maximum likelihood (ML) and Wiener filters for reconstructing noisy images taken through sparse-aperture telescopes. When the SNR is moderate or low, and Poisson-distributed photon noise dominates, then the quality of the imagery is significantly better for the ML reconstructions than for the Wiener filtered images. However, this does not happen for most realistic scenarios, and the ML algorithm has no advantage over the Wiener filter with regards to image quality. At lower SNRs, Poisson noise does not dominate over Gaussian noise, making the Wiener filter most appropriate. This is a result of the combined effects of (a) detector noise, which is Gaussian-distributed, (b) haze noise, which acts as though it were Gaussian, and (c) the fact that the raw images from sparse-aperture telescopes are low contrast. At higher SNRs, both classes of algorithms give similar results irrespective of the type of noise present. It is possible to concoct scenarios of moderate light levels, low-noise detectors, and excellent atmospheric conditions under which Poisson noise does dominate and the ML algorithm could produce images of significantly better quality than that from a Wiener filter. However, those scenarios would represent a small fraction of realistic cases of interest. Given the simpler computational requirements of the Wiener filter, it would ordinarily be preferred.

ACKNOWLEDGMENTS

Thanks for software support go to John Crowe. Helpful discussions with Richard Boucher, Robert Fiete, Edward Meinel, and Brian Thelen are gratefully acknowledged.

REFERENCES

- ¹ http://planetquest.jpl.nasa.gov/TPF/tpf_what_is.html
- ² J.R. Fienup, "MTF and Integration Time versus Fill Factor for Sparse-Aperture Imaging Systems," Proc. SPIE 4091A-06, Imaging Technology and Telescopes, San Diego, CA, 30 July 2000, pp. 43-47.
- ³ R. Fiete, "Modeling of Sparse Aperture Telescope Image Quality," in Integrated Computational Imaging Systems, Topical Meeting of the Optical Society of America, Albuquerque, NM, 6-8 November 2001, paper JW1.
- ⁴ C.W. Helstrom, "Image Restoration by the Method of Least Squares," J. Opt. Soc. Am. 57, 297-303 (1967).
- ⁵ J.R. Fienup, "Refined Wiener-Helstrom Image Reconstruction," Annual Meeting of the Optical Society of America, Long Beach, CA, October 18, 2001
- ⁶ B.R. Hunt, "Bayesian Methods in Nonlinear Digital Image Restoration," IEEE Trans. Comput. C-26, 511-518 (1972).
- ⁷ E.S. Meinel, "Origins of Linear and Nonlinear Recursive Restoration Algorithms," J. Opt. Soc. Am A 3, 787-799 (1986).
- ⁸ J.C. Leachtenauer, W. Malila, J. Irvine, L. Colburn, N. Salvaggio, "General Image-Quality Equation: GIQE," Appl. Opt. 36, 8322-8328 (1997).